JACS
JOURNAL OF THE AMERICAN CHEMICAL SOCIETY
Article
pubs.acs.org/JACS

A Hydrophobic Surface Is Essential To Inhibit the Aggregation of a Tau-Protein-Derived Hexapeptide

Jing Zheng, Arya M. Baghkhanian, and James S. Nowick*

Department of Chemistry, University of California, Irvine, Irvine, California 92697-2025, United States

Supporting Information

ABSTRACT: This paper seeks to understand how a macrocyclic β-sheet peptide inhibits the aggregation of the tau-protein-derived peptide Ac-VQIVYK-NH_2 (AcPHF6). Previous studies established that macrocyclic β-sheet peptide **1** inhibits AcPHF6 aggregation, while the sequence isomer in which the lysine and leucine residues at positions R_6 and R_7 are swapped has little effect on AcPHF6 aggregation. The current studies find that positions R_1, R_3, and R_7 are especially sensitive to mutations. Reducing hydrophobicity at these positions substantially diminishes inhibition. Although position R_5 is not sensitive to mutations that reduce hydrophobicity, it is sensitive to mutations that increase hydrophobicity. Enhanced hydrophobicity at this position substantially enhances inhibition. These studies establish that the hydrophobic surface comprising residues R_1, R_3, and R_7 is crucial to the inhibition process and that the residue R_5, which shares this surface, is also important. Collectively, these findings demonstrate that hydrophobic surfaces between β-sheet layers are important in inhibiting amyloid aggregation.

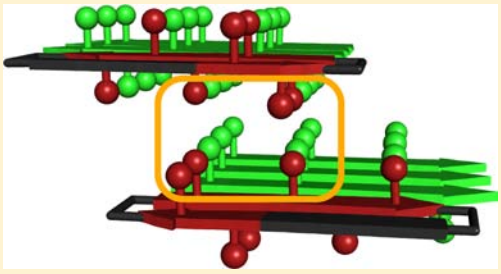

INTRODUCTION

The amyloidogenic hexapeptide sequence VQIVYK from the protein tau, which undergoes hyperphosphorylation and aggregates to form neurofibrillary tangles in Alzheimer's disease and certain frontotemporal dementias, provides an ideal model with which to explore the supramolecular chemistry of β-sheet aggregation and amyloid formation.[1] Both the sequence ^{306}VQIVYK^{311} in the third repeat domain and the homologous sequence ^{275}VQIINK^{280} in the second repeat domain are critical in nucleating the β-sheet aggregation of the entire protein.[2] The X-ray crystallographic structure of the peptide VQIVYK provides insights into the aggregation process by showing paired layers of parallel, in-register β-sheets similar to those of many other amyloids.[3−6] In this structure, the valine and isoleucine residues of the two β-sheet layers pack to form a hydrophobic core (Figure 1).

Goux et al. developed the acetylated peptide amide Ac-VQIVYK-NH_2 (AcPHF6) as a model system of tau protein aggregation and amyloid formation. AcPHF6 aggregates in buffer to form fibrils that resemble those formed by tau. Infrared spectroscopic studies suggest the fibrils contain parallel β-sheets,[7] like those seen for VQIVYK. The aggregation process can be studied by thioflavin S (ThS) fluorescence assays, like those used to study tau aggregation.[8] AcPHF6 aggregation occurs quickly, starting almost as soon as the assay is begun and reaching a maximum within 20 min.

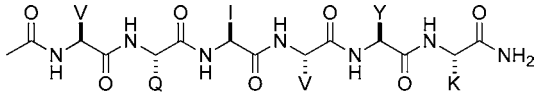

AcPHF6 (Ac-VQIVYK-NH_2)

We recently published studies of a series of macrocyclic β-sheet peptides that inhibit AcPHF6 aggregation.[9] The macrocycles contain a recognition strand (R_1−R_5), two additional residues on the lower strand (R_6 and R_7), a Hao molecular template to prevent further hydrogen-bonding interactions and aggregation, and two δ-linked ornithine residues as β-turn mimics.[10−12] Figure 2A illustrates the generic structure of macrocycle **1**. Figure 2B provides a simplified illustration of the macrocycle, showing residues R_1, R_3, R_5, and R_7 on the top surface of the β-sheet peptide and residues R_2, R_4, and R_6 on the bottom surface.

One of the best inhibitors, macrocycle **1**, slightly slowed aggregation of AcPHF6 at 0.25 equiv, substantially delayed aggregation at 0.5 equiv, and suppressed aggregation at 1.0 equiv for the duration of the assay (>100 min). Swapping the two residues on the lower strand to give macrocycle $\mathbf{1}_{K6L,L7K}$ resulted in a poor inhibitor. We nicknamed this macrocycle the "swapmer", because the hydrophilic lysine and hydrophobic leucine residues were swapped.[13] We proposed a model to explain the swapmer effect in which two molecules of the macrocycle cooperatively bind to the edges of small VQIVYK aggregates and inhibit further aggregation (Figure 3). The strongly nonlinear dependence of inhibition on the concentration of macrocycle **1** supports this model of cooperative inhibition by the macrocycle.

Here we set out to better understand why the swapmer is such a poor inhibitor and why macrocycle **1** is such a good inhibitor by systematically mutating the structure of macrocycle **1**. We began by replacing each of the R_1−R_7 residues with

Received: November 2, 2012
Published: April 29, 2013

dx.doi.org/10.1021/ja310817d | J. Am. Chem. Soc. 2013, 135, 6846−6852

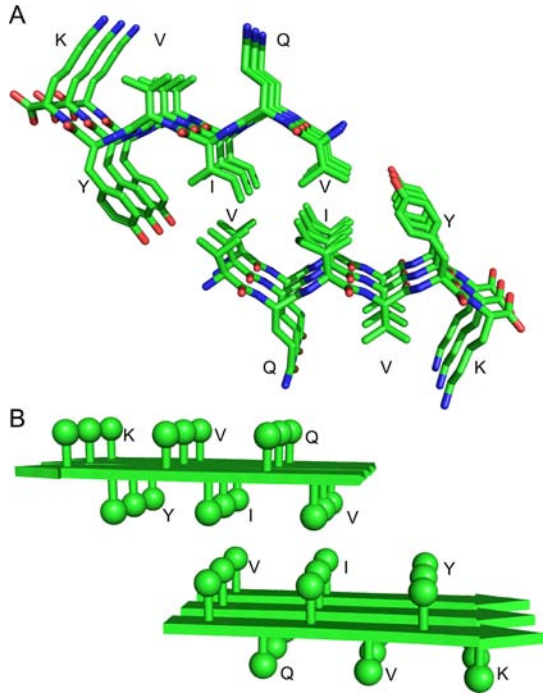

Figure 1. Solid-state structure of the VQIVYK peptide. (A) X-ray crystallographic structure showing three asymmetric units.[3] (B) Simplified illustration representing the peptides as idealized flat arrows and the side chains as balls and sticks.

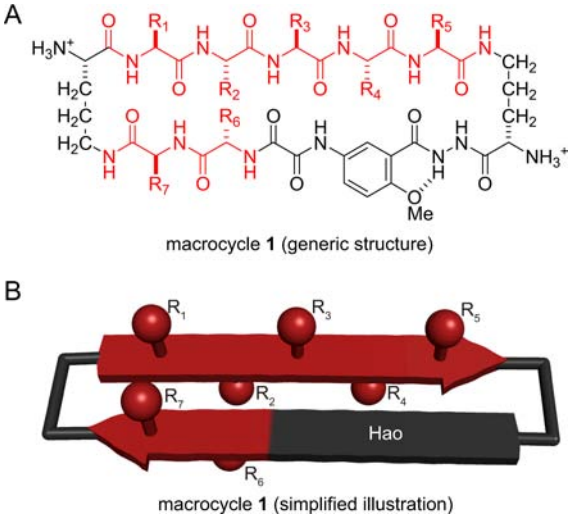

Figure 2. Structure of macrocycle **1**. (A) Line drawing. The upper strand (recognition) and the two additional residues on the lower strand are shown in red. The δ-linked ornithine turn units and Hao molecular template are shown in black. (B) Simplified illustration.

alanine to see the effects of diminishing the side chains. We then replaced the residues with serine to see the effects of replacing each residue with a hydrophilic group. We then focused on positions R_1, R_3, and R_7, which proved especially sensitive to these mutations, and explored the effects of residues with different hydrophobicity and size at these positions. Finally we performed additional mutations to explore the R_5 position. Collectively, these studies establish that a hydrophobic surface comprising residues R_1, R_3, and R_7 is necessary for inhibition and that residue R_5, which shares this surface, is also important.

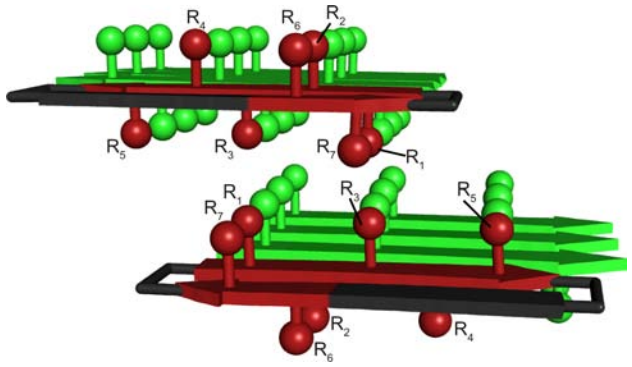

Figure 3. Illustration of two macrocycles bound to the edges of the layered β-sheets of the VQIVYK peptide.

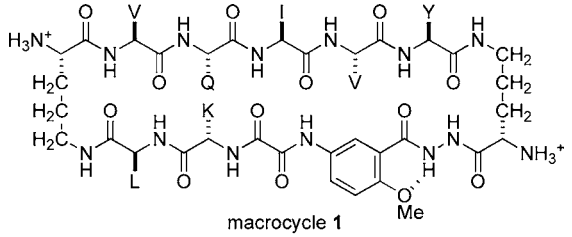

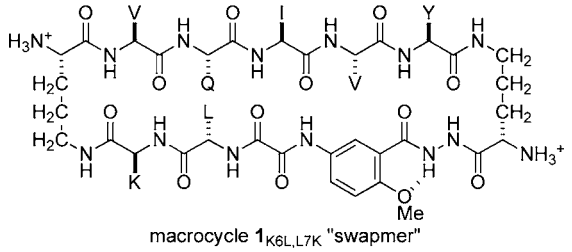

RESULTS AND DISCUSSION

1. Alanine Scan of Macrocycle 1. To explore which residues are important in inhibiting the aggregation of AcPHF6, we synthesized seven mutants of macrocycle **1** in which each of the seven residues was replaced with alanine. The sequences of these macrocycles are shown in Table 1. In macrocycle $\mathbf{1}_{V1A}$, the valine at the R_1 position, on the top surface of the β-sheet, is mutated to alanine. In macrocycle $\mathbf{1}_{Q2A}$, the glutamine at the R_2 position, on the bottom surface of the β-sheet, is mutated to alanine. Macrocycles $\mathbf{1}_{I3A}$, $\mathbf{1}_{V4A}$, $\mathbf{1}_{Y5A}$, $\mathbf{1}_{K6A}$, and $\mathbf{1}_{L7A}$ are similarly named and alternately vary the residues on the top and bottom surfaces of the β-sheet.

The effects of the macrocycles on AcPHF6 aggregation were studied with ThS fluorescence assays in which 100 μM AcPHF6 is allowed to aggregate in 16 mM MOPS buffer. Thioflavin S exhibits increasing fluorescence as it interacts with the aggregates that form. Each experiment was performed in triplicate in 96-well plates, and the experiments were repeated to ensure reproducibility. Figure 4A shows a typical set of experiments in which AcPHF6 is allowed to aggregate with and without added macrocycle **1**. Without any added macrocycle, fluorescence increases rapidly and reaches a maximum within 20 min (black curve in Figure 4A). The rapid increase in fluorescence indicates that AcPHF6 aggregates immediately upon setting up the plate and beginning the experiment. Addition of 25 μM macrocycle **1** slightly slows aggregation (red curve in Figure 4A). Addition of 50 μM macrocycle **1**

dx.doi.org/10.1021/ja310817d | J. Am. Chem. Soc. 2013, 135, 6846−6852

Table 1. Alanine-Scan Mutants of Macrocycle 1

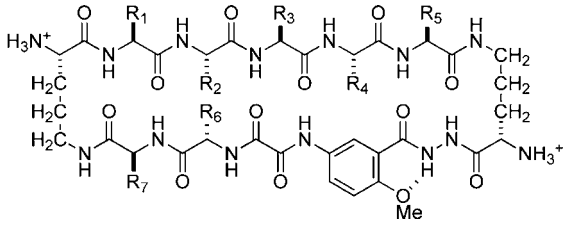

macrocycle	R_1	R_2	R_3	R_4	R_5	R_6	R_7
1	Val	Gln	Ile	Val	Tyr	Lys	Leu
$\mathbf{1}_{V1A}$	Ala	Gln	Ile	Val	Tyr	Lys	Leu
$\mathbf{1}_{Q2A}$	Val	Ala	Ile	Val	Tyr	Lys	Leu
$\mathbf{1}_{I3A}$	Val	Gln	Ala	Val	Tyr	Lys	Leu
$\mathbf{1}_{V4A}$	Val	Gln	Ile	Ala	Tyr	Lys	Leu
$\mathbf{1}_{Y5A}$	Val	Gln	Ile	Val	Ala	Lys	Leu
$\mathbf{1}_{K6A}$	Val	Gln	Ile	Val	Tyr	Ala	Leu
$\mathbf{1}_{L7A}$	Val	Gln	Ile	Val	Tyr	Lys	Ala

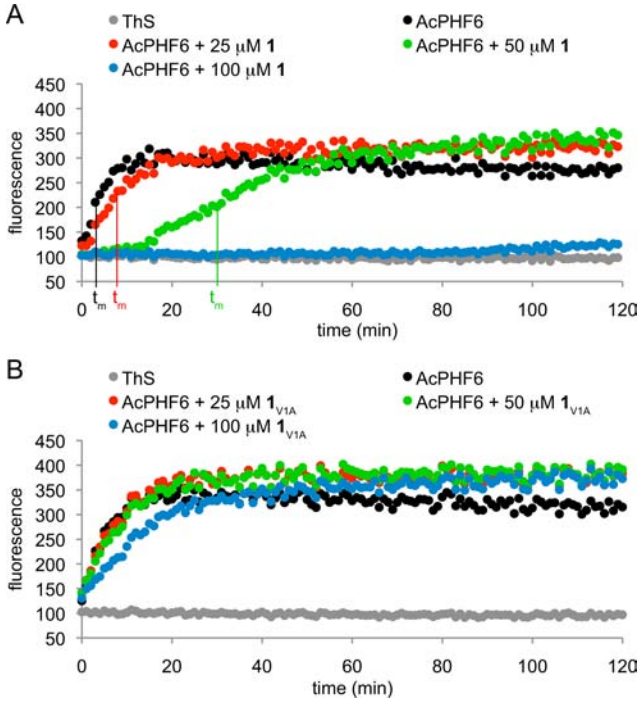

Figure 4. (A) Aggregation of 100 μM AcPHF6 in the absence and presence of 25, 50, and 100 μM of macrocycle **1**. The t_m values of the black, red, and green curves are marked. (B) Aggregation of 100 μM AcPHF6 in the absence and presence of 25, 50, and 100 μM of macrocycle $\mathbf{1}_{V1A}$. Each experiment was run in triplicate in a 96-well plate. Representative data from individual experiments are shown above. For graphs of all experiments, see the Supporting Information.

substantially delays aggregation (green curve in Figure 4A). Addition of 100 μM macrocycle **1** suppresses aggregation for the duration of the assay (blue curve in Figure 4A).

Figure 4B shows a set of experiments in which AcPHF6 is allowed to aggregate with and without added macrocycle $\mathbf{1}_{V1A}$. Macrocycle $\mathbf{1}_{V1A}$ is a much poorer inhibitor of AcPHF6 aggregation than macrocycle **1**. Addition of 25 μM or 50 μM macrocycle $\mathbf{1}_{V1A}$ has little or no effect on AcPHF6 aggregation, and addition of 100 μM macrocycle $\mathbf{1}_{V1A}$ only slightly slows the aggregation (Figure 4B). Thus, the decrease in size and hydrophobicity of the R_1 residue on the top surface of the

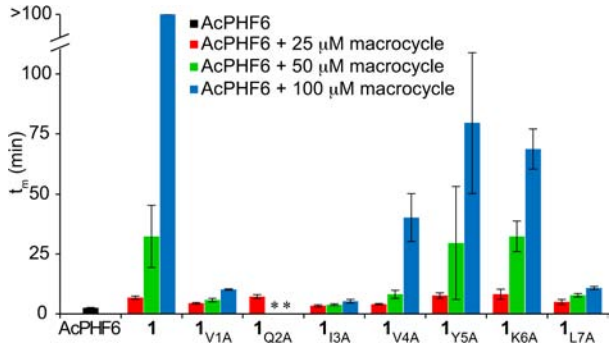

Figure 5. Effects of macrocycle **1** and the seven alanine mutants on AcPHF6 aggregation. The error bars show standard deviations among triplicate experiments. *The t_m for 50 and 100 μM macrocycle $\mathbf{1}_{Q2A}$ were not determined because the macrocycle appears to aggregate at higher concentrations under the ThS assay conditions, even in the absence of AcPHF6.

β-sheet from an isopropyl group to a methyl group dramatically attenuates the inhibition.

The time corresponding to the midpoint of fluorescence relative to the ThS control (t_m, Figure 4A) provides a convenient index of the effects of the different macrocycles on AcPHF6 aggregation.[14] Without any macrocycle, the t_m is 2.3 $\pm$ 0.4 min (average and standard deviation of three experiments in a 96-well plate). With 25 μM macrocycle **1**, t_m increases to 6.8 $\pm$ 0.7 min. With 50 μM macrocycle **1**, t_m further increases to 32.4 $\pm$ 13.0 min.[15] With 100 μM macrocycle **1**, t_m is greater than the duration of the assay (>100 min). In contrast, macrocycle $\mathbf{1}_{V1A}$ exhibits shorter t_m values of 4.5 $\pm$ 0.3, 5.8 $\pm$ 0.7, and 10.2 $\pm$ 0.2 min at 25, 50, and 100 μM respectively.

Figure 5 presents these data graphically. The short black bar on the left side of the graph illustrates t_m for AcPHF6 alone. The adjacent set of red, green, and blue bars correspond to t_m for 25, 50, and 100 μM added macrocycle **1**. The next set of red, green, and blue bars corresponds to 25, 50, and 100 μM added macrocycle $\mathbf{1}_{V1A}$. The remaining sets correspond to the other alanine mutants.

Macrocycles $\mathbf{1}_{Y5A}$ and $\mathbf{1}_{K6A}$ are both good inhibitors of AcPHF6 aggregation (Figure 5). Like macrocycle **1**, these macrocycles show substantial increases in t_m at 50 and 100 μM and smaller increases in t_m at 25 μM. Macrocycle $\mathbf{1}_{V4A}$ shows moderate reduction in inhibition compared to macrocycle **1** especially at 50 and 100 μM. Macrocycles $\mathbf{1}_{V1A}$, $\mathbf{1}_{I3A}$, and $\mathbf{1}_{L7A}$ are much poorer inhibitors than macrocycle **1**, showing smaller increases in t_m at 50 and 100 μM. Macrocycle $\mathbf{1}_{Q2A}$ aggregates under the conditions of the assay at 50 and 100 μM and is thus difficult to compare to the other sets of experiments. At 25 μM, macrocycle $\mathbf{1}_{Q2A}$ significantly slows aggregation (t_m = 7.2 $\pm$ 0.8 min) and thus appears to be similar to macrocycle **1** as a good inhibitor. We performed additional serine-scan experiments to corroborate this result in section 2.

The short t_m of macrocycles $\mathbf{1}_{V1A}$, $\mathbf{1}_{I3A}$, and $\mathbf{1}_{L7A}$ suggest that the residues valine, isoleucine, and leucine at the R_1, R_3, and R_7 positions on the top surface of the β-sheet of macrocycle **1** are especially important in the inhibition process. In contrast, the relatively long t_m of macrocycles $\mathbf{1}_{V4A}$ and $\mathbf{1}_{K6A}$ suggest the R_4 valine and the R_6 lysine on the bottom surface of the β-sheet are less important. The long t_m of macrocycle $\mathbf{1}_{Y5A}$ suggests that the R_5 tyrosine on the top surface is also less important. While only limited data are available for macrocycle $\mathbf{1}_{Q2A}$, the

dx.doi.org/10.1021/ja310817d | J. Am. Chem. Soc. 2013, 135, 6846−6852

Table 2. Serine-Scan Mutants of Macrocycle 1

macrocycle	R_1	R_2	R_3	R_4	R_5	R_6	R_7
$\mathbf{1}_{V1S}$	Ser	Gln	Ile	Val	Tyr	Lys	Leu
$\mathbf{1}_{Q2S}$	Val	Ser	Ile	Val	Tyr	Lys	Leu
$\mathbf{1}_{I3S}$	Val	Gln	Ser	Val	Tyr	Lys	Leu
$\mathbf{1}_{V4S}$	Val	Gln	Ile	Ser	Tyr	Lys	Leu
$\mathbf{1}_{Y5S}$	Val	Gln	Ile	Val	Ser	Lys	Leu
$\mathbf{1}_{K6S}$	Val	Gln	Ile	Val	Tyr	Ser	Leu
$\mathbf{1}_{L7S}$	Val	Gln	Ile	Val	Tyr	Lys	Ser

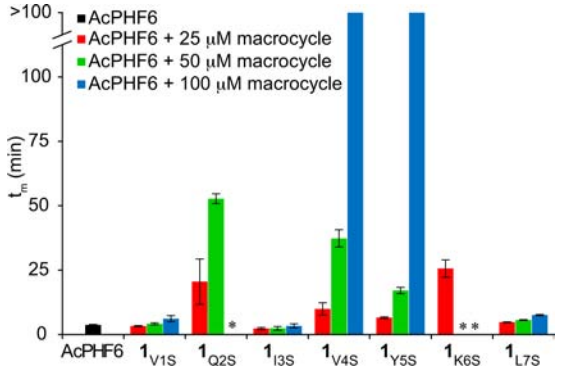

Figure 6. Effects of the seven serine mutants on AcPHF6 aggregation. The error bars show standard deviations among triplicate experiments. *The t_m for 100 μM macrocycle $\mathbf{1}_{Q2S}$ and 50 and 100 μM macrocycle $\mathbf{1}_{K6S}$ were not determined because the macrocycles appear to aggregate at higher concentrations under the ThS assay conditions, even in the absence of AcPHF6.

similarity of t_m at 25 μM to that of macrocycle **1** suggests that the R_2 glutamine is also less important. These results are consistent with the model in Figure 3, in which the hydrophobic top surface of the macrocycle is essential in the inhibition process. The R_1, R_3, and R_7 residues on the top surface of the β-sheet of the macrocycle align with the central hydrophobic core of the layered β-sheets of the VQIVYK peptide, and thus, these residues are sensitive to alanine mutation. The R_5 residue shares this top surface but is out of the hydrophobic core, and thus, it is insensitive to alanine mutation.

2. Serine Scan of Macrocycle 1. To corroborate these findings and address the problem with limited data from $\mathbf{1}_{Q2A}$, we performed additional experiments by replacing each of the seven residues of macrocycle **1** with serine. The sequences of these macrocycles are shown in Table 2. Figure 6 shows the effects of these macrocycles on AcPHF6 aggregation. Macrocycles $\mathbf{1}_{V4S}$ and $\mathbf{1}_{Y5S}$ are both good inhibitors of AcPHF6 aggregation. Like macrocycle **1**, these macrocycles show substantial increases in t_m at 50 and 100 μM and smaller increases in t_m at 25 μM. Macrocycles $\mathbf{1}_{V1S}$, $\mathbf{1}_{I3S}$, and $\mathbf{1}_{L7S}$ are much poorer inhibitors than macrocycle **1**, showing at most small increases in t_m at 25, 50, and 100 μM. Macrocycle $\mathbf{1}_{Q2S}$ aggregates under the conditions of the assay at 100 μM, but the substantial increases in t_m at 25 and 50 μM strongly suggest that macrocycle $\mathbf{1}_{Q2S}$ is a good inhibitor. Macrocycle $\mathbf{1}_{K6S}$ aggregates under the conditions of the assay at 50 and 100 μM. At 25 μM, macrocycle $\mathbf{1}_{K6S}$ shows a significant increase in t_m and thus also appears to be a good inhibitor.

The diminished inhibition of macrocycles $\mathbf{1}_{V1S}$, $\mathbf{1}_{I3S}$, and $\mathbf{1}_{L7S}$ corroborates that the residues valine, isoleucine, and leucine at the R_1, R_3, and R_7 positions on the top surface of the β-sheet of macrocycle **1** are especially important in the inhibition process. Replacing these hydrophobic residues with a hydrophilic serine residue is detrimental to the inhibition. These results are consistent with the results from the alanine-scan experiments that macrocycles $\mathbf{1}_{V1A}$, $\mathbf{1}_{I3A}$, and $\mathbf{1}_{L7A}$ are much poorer inhibitors than macrocycle **1**. In contrast, the long t_m of macrocycles $\mathbf{1}_{V4S}$ and $\mathbf{1}_{Y5S}$ suggest the R_4 valine on the bottom surface of the β-sheet and the R_5 tyrosine on the top surface of the β-sheet are less important. The substantial increases in t_m at 25 and 50 μM $\mathbf{1}_{Q2S}$ suggests that the R_2 glutamine on the bottom surface is also less important. While only limited data are available for macrocycle $\mathbf{1}_{K6S}$, the substantial increase in t_m at 25 μM $\mathbf{1}_{K6S}$, along with the previous results of macrocycle $\mathbf{1}_{K6A}$, suggests that the R_6 lysine on the bottom surface is also less important. The sensitivity of the R_1–R_7 residues to alanine and serine mutations is summarized in Table 3. Collectively, these findings from the alanine and serine scans support a model in which the hydrophobic top surface of the macrocycle is essential in the inhibition process.

Table 3. Sensitivity of the R_1–R_7 Residues to Alanine and Serine Mutations

position	sensitivity
R_1	**sensitive**
R_2	not sensitive
R_3	**sensitive**
R_4	not sensitive
R_5	not sensitive
R_6	not sensitive
R_7	**sensitive**

3. Effect of the R_1 Residue. To further investigate the sensitivity of the R_1 position to mutation, we systematically changed the size and hydrophobicity of the residue at the R_1 position (Table 4). The valine-to-alanine mutant $\mathbf{1}_{V1A}$ has a smaller, less hydrophobic R_1 residue. The valine-to-cyclohexylglycine mutant $\mathbf{1}_{V1Chg}$ has a larger, more hydrophobic R_1 residue. The valine-to-threonine mutant $\mathbf{1}_{V1T}$ has a hydrophilic R_1 residue that is comparable in size to valine. Figure 7 shows the effects of these macrocycles on AcPHF6 aggregation. Macrocycles $\mathbf{1}_{V1A}$ and $\mathbf{1}_{V1T}$ are much poorer inhibitors than macrocycle **1**, showing small increases in t_m at 25, 50, and 100 μM. Macrocycle $\mathbf{1}_{V1Chg}$ appears to be a slightly better inhibitor than macrocycle **1**. Addition of 50 μM $\mathbf{1}_{V1Chg}$ suppresses aggregation for the duration of the assay (>100 min), while addition of 50 μM **1** only delays aggregation.

These results further demonstrate that the R_1 residue on the top surface is important in inhibition. The valine-to-alanine mutation diminishes the size and hydrophobicity of the R_1 residue and disrupts the interlayer hydrophobic interactions. Cyclohexylglycine is bigger and more hydrophobic than valine and augments the hydrophobicity of the top surface. The hydrophobic core appears to accommodate the larger size of the Chg side chain.[16] Threonine is hydrophilic and disrupts the interlayer hydrophobic interactions, and thus the valine-to-threonine mutation results in a much poorer inhibitor.

4. Effect of the R_3 Residue. We investigated the sensitivity of the R_3 position to mutation by systematically changing the size and hydrophobicity of the residue at the R_3 position in a similar fashion (Table 5). In addition to alanine, valine, cyclohexylglycine, and threonine, we also mutated the original isoleucine residue to the diastereomeric hydrophobic residue alloisoleucine. Figure 8 shows the effects of these macrocycles

dx.doi.org/10.1021/ja310817d | J. Am. Chem. Soc. 2013, 135, 6846–6852

Table 4. R_1 Mutants of Macrocycle 1

macrocycle	R_1	R_2	R_3	R_4	R_5	R_6	R_7
1	Val	Gln	Ile	Val	Tyr	Lys	Leu
$\mathbf{1}_{V1A}$	Ala	Gln	Ile	Val	Tyr	Lys	Leu
$\mathbf{1}_{V1Chg}$	Chg	Gln	Ile	Val	Tyr	Lys	Leu
$\mathbf{1}_{V1T}$	Thr	Gln	Ile	Val	Tyr	Lys	Leu

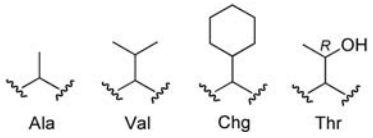

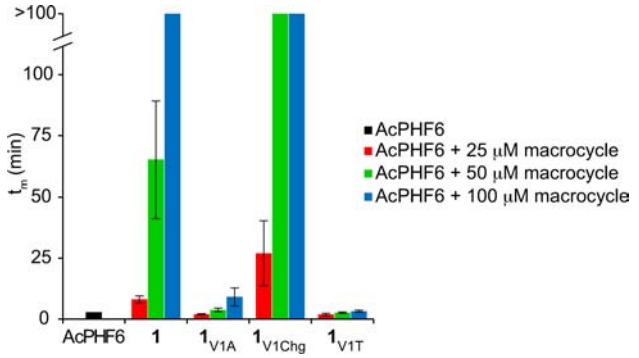

Figure 7. Effects of macrocycles **1**, $\mathbf{1}_{V1A}$, $\mathbf{1}_{V1Chg}$, and $\mathbf{1}_{V1T}$ on AcPHF6 aggregation. The error bars show standard deviations among triplicate experiments.

on AcPHF6 aggregation. Macrocycles $\mathbf{1}_{I3V}$, $\mathbf{1}_{I3Chg}$, and $\mathbf{1}_{I3Ail}$ are all good inhibitors of AcPHF6 aggregation. Like macrocycle **1**, macrocycles $\mathbf{1}_{I3Chg}$ and $\mathbf{1}_{I3Ail}$ show substantial increases in t_m at 50 and 100 μM and a smaller increase in t_m at 25 μM. Macrocycle $\mathbf{1}_{I3V}$ shows a substantial increase in t_m at 100 μM and smaller increases in t_m at 25 and 50 μM. In contrast, macrocycles $\mathbf{1}_{I3A}$ and $\mathbf{1}_{I3T}$ are much poorer inhibitors than macrocycle **1**, showing only small increases in t_m at 25, 50, and 100 μM.

These results further demonstrate that the R_3 residue on the top surface of the β-sheet of the macrocycle is essential in the inhibition process. Macrocycle $\mathbf{1}_{I3V}$ is a good inhibitor but shows a shorter t_m at 50 μM than that of **1**. This difference may reflect that valine is slightly smaller and less hydrophobic than isoleucine. Macrocycles $\mathbf{1}_{I3Chg}$ and $\mathbf{1}_{I3Ail}$ are good inhibitors, like macrocycle **1**, because cyclohexylglycine and alloisoleucine are both large and hydrophobic, like isoleucine. The similarity between **1** and $\mathbf{1}_{I3Ail}$ suggests that the stereochemistry of the R_3 residue is not important in inhibition. Alanine is much smaller and less hydrophobic than isoleucine, and thus macrocycle $\mathbf{1}_{I3A}$ is a much poorer inhibitor. Threonine is hydrophilic, and disrupts the interlayer hydrophobic interactions. Collectively, these results establish that, like residue R_1, the hydrophobicity of residue R_3 on the top surface of the β-sheet is essential in the inhibition process.

5. Effect of the R_7 Residue. We investigated the sensitivity of the R_7 position to mutation by systematically changing the size and hydrophobicity of the residue at the R_7 position in a similar fashion (Table 6). In addition to alanine, valine, and threonine, we also mutated the original leucine residue to tyrosine and phenylalanine. Figure 9 shows the effects of these macrocycles on AcPHF6 aggregation. Macrocycle $\mathbf{1}_{L7V}$ is a good inhibitor of AcPHF6 aggregation, showing a substantial

Table 5. R_3 Mutants of Macrocycle 1

macrocycle	R_1	R_2	R_3	R_4	R_5	R_6	R_7
1	Val	Gln	Ile	Val	Tyr	Lys	Leu
$\mathbf{1}_{I3A}$	Val	Gln	Ala	Val	Tyr	Lys	Leu
$\mathbf{1}_{I3V}$	Val	Gln	Val	Val	Tyr	Lys	Leu
$\mathbf{1}_{I3Chg}$	Val	Gln	Chg	Val	Tyr	Lys	Leu
$\mathbf{1}_{I3T}$	Val	Gln	Thr	Val	Tyr	Lys	Leu
$\mathbf{1}_{I3Ail}$	Val	Gln	Ail	Val	Tyr	Lys	Leu

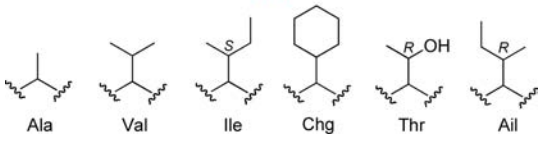

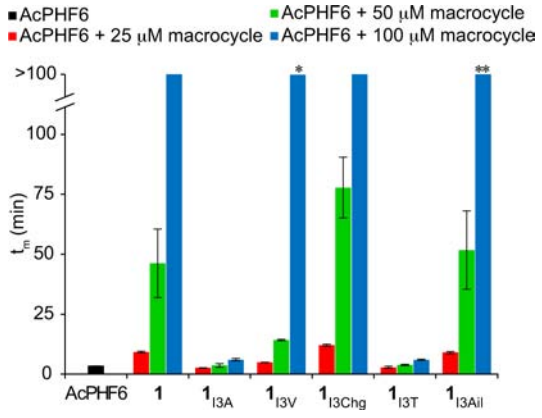

Figure 8. Effects of macrocycles **1**, $\mathbf{1}_{I3A}$, $\mathbf{1}_{I3V}$, $\mathbf{1}_{I3Chg}$, $\mathbf{1}_{I3T}$, and $\mathbf{1}_{I3Ail}$ on AcPHF6 aggregation. The error bars show standard deviations among triplicate experiments. *With 100 μM added $\mathbf{1}_{I3V}$, two runs show suppression of AcPHF6 aggregation for the duration of the assay and one run shows a delay in AcPHF6 aggregation. For details, see Figure S4, Part 3, in the Supporting Information. **With 100 μM added $\mathbf{1}_{I3Ail}$, the data appear largely consistent with suppression, although a slight increase in fluorescence occurs at about 30 min. For details, see Figure S4, Part 6, in the Supporting Information.

increase in t_m at 100 μM and smaller increases in t_m at 25 and 50 μM. Macrocycle $\mathbf{1}_{L7Y}$ shows shorter t_m values at 25, 50, and 100 μM than those of macrocycle **1**, and thus is a modest inhibitor compared to **1** and $\mathbf{1}_{L7V}$. Macrocycle $\mathbf{1}_{L7F}$ aggregates under the conditions of the assay at 100 μM. At 25 and 50 μM, macrocycle $\mathbf{1}_{L7F}$ substantially increases t_m, suggesting that it is a good inhibitor, like macrocycle **1**. Macrocycles $\mathbf{1}_{L7A}$ and $\mathbf{1}_{L7T}$ are much poorer inhibitors than **1**, showing only small increases in t_m at 25, 50, and 100 μM.

These results further demonstrate that the R_7 residue on the top surface of the β-sheet of the macrocycle is essential in the inhibition process. Macrocycle $\mathbf{1}_{L7V}$ is a good inhibitor but shows a shorter t_m at 50 μM than that of macrocycle **1**. This difference may reflect that valine is smaller and less hydrophobic than leucine. The leucine-to-alanine mutation diminishes the size and hydrophobicity of the R_7 residue, and the leucine-to-threonine mutation results in a hydrophilic residue at position R_7, and thus both $\mathbf{1}_{L7A}$ and $\mathbf{1}_{L7T}$ are much poorer inhibitors than **1**. Macrocycle $\mathbf{1}_{L7Y}$ is a modest inhibitor, likely due to the hydrophilic hydroxyl group on the tyrosine residue. Macrocycle $\mathbf{1}_{L7F}$ appears to be a better inhibitor, likely because phenylalanine lacks the hydroxyl group and is thus more hydrophobic. Collectively, these results establish that, like the R_1 and R_3 residues, the hydrophobicity of the R_7 residue on the top surface of the β-sheet is essential in the inhibition process.

dx.doi.org/10.1021/ja310817d | J. Am. Chem. Soc. 2013, 135, 6846−6852

Table 6. R_7 Mutants of Macrocycle 1

macrocycle	R_1	R_2	R_3	R_4	R_5	R_6	R_7
1	Val	Gln	Ile	Val	Tyr	Lys	Leu
$\mathbf{1}_{L7A}$	Val	Gln	Ile	Val	Tyr	Lys	Ala
$\mathbf{1}_{L7V}$	Val	Gln	Ile	Val	Tyr	Lys	Val
$\mathbf{1}_{L7T}$	Val	Gln	Ile	Val	Tyr	Lys	Thr
$\mathbf{1}_{L7Y}$	Val	Gln	Ile	Val	Tyr	Lys	Tyr
$\mathbf{1}_{L7F}$	Val	Gln	Ile	Val	Tyr	Lys	Phe

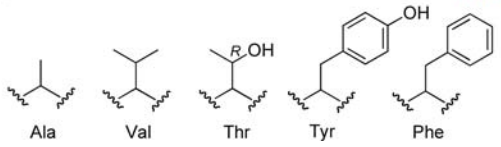

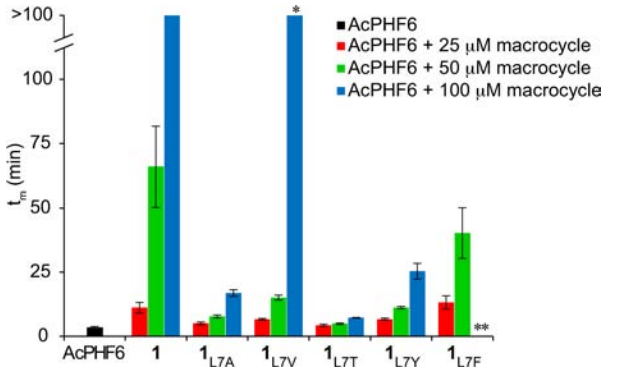

Figure 9. Effects of macrocycles **1**, $\mathbf{1}_{L7A}$, $\mathbf{1}_{L7V}$, $\mathbf{1}_{L7T}$, $\mathbf{1}_{L7Y}$, and $\mathbf{1}_{L7F}$ on AcPHF6 aggregation. The error bars show standard deviations among triplicate experiments. *With 100 μM added $\mathbf{1}_{L7V}$, two runs show suppression of AcPHF6 aggregation for the duration of the assay and one run shows a delay in AcPHF6 aggregation. For details, see Figure S5, Part 3, in the Supporting Information. **The t_m for 100 μM macrocycle $\mathbf{1}_{L7F}$ was not determined because the macrocycle appears to aggregate at higher concentrations under the ThS assay conditions, even in the absence of AcPHF6.

6. Effect of the R_5 Residue. The tyrosine residue at the R_5 position is not sensitive to alanine or serine mutation. We further explored the R_5 position by replacing the tyrosine residue with phenylalanine and *O*-methyltyrosine, which lack the hydrophilic hydroxyl group (Table 7). Figure 10 shows the effects of these macrocycles on AcPHF6 aggregation. Macrocycles $\mathbf{1}_{Y5F}$ and $\mathbf{1}_{Y5Y(Me)}$ show much stronger inhibition than macrocycle **1**, especially at very low substoichiometric concentrations (10–25 μM). Both macrocycles show a small increase in t_m at 5 μM, a substantial increase in t_m at 10 μM, and suppress AcPHF6 aggregation at 15 μM. In contrast, macrocycle **1** shows no significant effect at 5 μM and only small increases in t_m at 10, 15, and 25 μM.

The enhanced activity of macrocycles $\mathbf{1}_{Y5F}$ and $\mathbf{1}_{Y5Y(Me)}$ suggests that increasing the hydrophobicity of the R_5 tyrosine may allow additional interlayer hydrophobic contacts that enhance inhibition. Although changing the tyrosine to alanine or serine does not significantly reduce inhibition, eliminating the hydrophilic hydroxyl group at the tip of the R_5 tyrosine results in a greater hydrophobic top surface and much better inhibitors. The enhanced hydrophobicity of the top surface of these macrocycles enhances the cooperativity of inhibition and allows macrocycles $\mathbf{1}_{Y5F}$ and $\mathbf{1}_{Y5Y(Me)}$ to show substantial increases in t_m at 0.1 equivalents and suppression of the aggregation at 0.15 equiv.

Table 7. R_5 Mutants of Macrocycle 1

macrocycle	R_1	R_2	R_3	R_4	R_5	R_6	R_7
1	Val	Gln	Ile	Val	Tyr	Lys	Leu
$\mathbf{1}_{Y5F}$	Val	Gln	Ile	Val	Phe	Lys	Leu
$\mathbf{1}_{Y5Y(Me)}$	Val	Gln	Ile	Val	Tyr(Me)	Lys	Leu

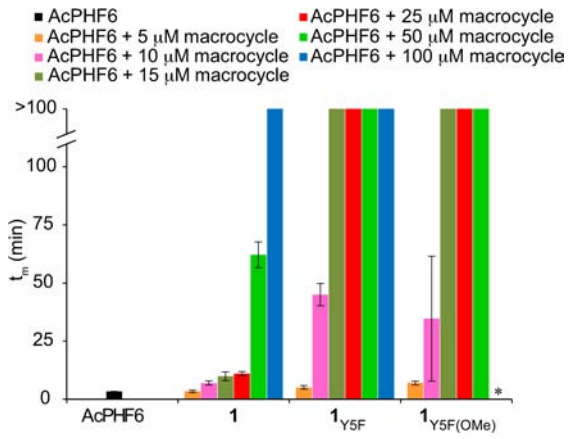

Figure 10. Effects of macrocycles **1**, $\mathbf{1}_{Y5F}$, and $\mathbf{1}_{Y5Y(Me)}$ on AcPHF6 aggregation. The error bars show standard deviations among triplicate experiments. *The t_m for 100 μM macrocycle $\mathbf{1}_{Y5Y(Me)}$ was not determined because the macrocycle appears to aggregate at higher concentrations under the ThS assay conditions, even in the absence of AcPHF6.

■ CONCLUSIONS

Macrocyclic β-sheet peptide **1** and suitable homologues effectively inhibits aggregation of the tau-protein-derived peptide AcPHF6. The hydrophobic surface created by the valine, isoleucine, and leucine residues at positions R_1, R_3, and R_7 on macrocycle **1** is necessary for inhibition (orange box in Figure 11). Mutating any of these residues to the less hydrophobic residues alanine, serine, or threonine greatly diminishes inhibition. The tyrosine residue at position R_5 that shares this surface is also important in the inhibition process. While mutating it to smaller, less hydrophobic residues has little effect on inhibition, increasing its hydrophobicity by eliminating the hydroxyl group enhances inhibition. Mutating the glutamine, valine, and lysine residues at positions R_2, R_4, and R_6 on the opposing surface of macrocycle **1** has little effect upon inhibition, although mutating the R_2 and R_6 residues tends to promote aggregation of the macrocycle under the ThS assay conditions.

While a variety of studies have probed the effects of different peptides in inhibiting amyloid aggregation, to our knowledge, none of these studies provide the sort of detailed insights into the inhibition process afforded by the current study.[17,18] Our study demonstrates that hydrophobic surfaces between the β-sheet layers are important in inhibiting amyloid aggregation. This principle should be applicable to larger amyloids such as those formed by full-length tau protein or β-amyloid peptides. Unlike these larger amyloids, the AcPHF6 model system lacks the conformational ambiguities of larger amyloidogenic peptides and thus allows the aggregation process to be studied in exquisite detail.[19,20] The macrocyclic β-sheet peptides provide two well-defined surfaces to display amino acid side chains and thus should be useful in future studies of amyloid inhibition and inhibitor design.

dx.doi.org/10.1021/ja310817d | J. Am. Chem. Soc. 2013, 135, 6846–6852

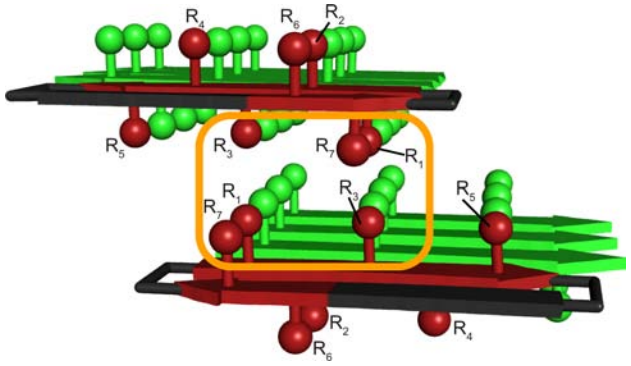

Figure 11. Illustration of two macrocycles bound to the edge of the layered β-sheets of the VQIVYK peptide. The orange box highlights the R_1, R_3, and R_7 residues of the macrocycles, which form a hydrophobic core and are essential to inhibition.

EXPERIMENTAL SECTION

Sample Preparation. All macrocycles were synthesized and purified according to published procedures[9,12] and characterized by analytical reversed-phase HPLC, electrospray mass spectrometry, and one-dimensional ^{1}H NMR spectroscopy. ^{1}H NMR experiments were performed on 2 mM solutions in D_2O. Each macrocycle showed suitable purity, with a single sharp peak in analytical RP-HPLC, peaks in the mass spectra associated with molecular ions, and sharp, well-defined peaks in the NMR spectra.

ThS Fluorescence Assays. ThS fluorescence assays were performed as described previously,[9] with the exception that aliquots of MOPS buffer, ThS solution, H_2O, and macrocycle solution were premixed in Eppendorf tubes and then divided into three wells of the 96-well plate. Aliquots of AcPHF6 solution were then added to each well, and the assay was begun immediately. For details, see the Supporting Information.

The time corresponding to the midpoint of fluorescence relative to the ThS control (t_m) was calculated for each experiment as follows: (1) For each data set, the last 10 readings of fluorescence signal were averaged to give a final fluorescence value F_{final}. (2) The last 10 readings of ThS background fluorescence were averaged to give a background fluorescence value F_{blank}. (3) The midpoint of aggregation was then identified as the time at which the fluorescence reaches $^1/_2(F_{final} + F_{blank})$.

ASSOCIATED CONTENT

Supporting Information

Procedures for ThS fluorescence assays, raw data traces of the ThS fluorescence assays from all experiments in the Results and Discussion, data tables of t_m values from these experiments, procedures for ^{1}H NMR experiments, and ^{1}H NMR spectra of all macrocycles. This material is available free of charge via the Internet at http://pubs.acs.org.

AUTHOR INFORMATION

Corresponding Author

jsnowick@uci.edu

Notes

The authors declare no competing financial interest.

ACKNOWLEDGMENTS

J.S.N. and J.Z. thank the NSF (CHE-1112188) for grant support. A.M.B. thanks the Allergan Foundation for an Allergan Summer Undergraduate Research Fellowship.

REFERENCES

(1) Mandelkow, E.; von Bergen, M.; Biernat, J.; Mandelkow, E. M. *Brain Pathol.* **2007**, *17*, 83−90.
(2) von Bergen, M.; Friedhoff, P.; Biernat, J.; Heberle, J.; Mandelkow, E. M.; Mandelkow, E. *Proc. Natl. Acad. Sci. U.S.A.* **2000**, *97*, 5129−5134.
(3) Sawaya, M. R.; Sambashivan, S.; Nelson, R.; Ivanova, M. I.; Sievers, S. A.; Apostol, M. I.; Thompson, M. J.; Balbirnie, M.; Wiltzius, J. J.; McFarlane, H. T.; Madsen, A. O.; Riekel, C.; Eisenberg, D. *Nature* **2007**, *447*, 453−457.
(4) Petkova, A. T.; Yau, W. M.; Tycko, R. *Biochemistry* **2006**, *45*, 498−512.
(5) Walsh, P.; Simonetti, K.; Sharpe, S. *Structure* **2009**, *17*, 417−426.
(6) A recent solid-state NMR study of tau fibrils reveals that the VQIVYK sequence is located in the β-sheet core of the fibril, and this core region shows parallel, in-register β-sheet structure. Daebel, V.; Chinnathambi, S.; Biernat, J.; Schwalbe, M.; Habenstein, B.; Loquet, A.; Akoury, E.; Tepper, K.; Müller, H.; Baldus, M.; Griesinger, C.; Zweckstetter, M.; Mandelkow, E.; Vijayan, V.; Lange, A. *J. Am. Chem. Soc.* **2012**, *134*, 13982−13989.
(7) Goux, W. J.; Kopplin, L.; Nguyen, A. D.; Leak, K.; Rutkofsky, M.; Shanmuganandam, V. D.; Sharma, D.; Inouye, H.; Kirschner, D. A. *J. Biol. Chem.* **2004**, *279*, 26868−26875.
(8) Friedhoff, P.; Schneider, A.; Mandelkow, E. M.; Mandelkow, E. *Biochemistry* **1998**, *37*, 10223−10230.
(9) Zheng, J.; Liu, C.; Sawaya, M. R.; Vadla, B.; Khan, S.; Woods, R. J.; Eisenberg, D.; Goux, W. J.; Nowick, J. S. *J. Am. Chem. Soc.* **2011**, *133*, 3144−3157.
(10) Nowick, J. S.; Lam, K. S.; Khasanova, T. V.; Kemnitzer, W. E.; Maitra, S.; Mee, H. T.; Liu, R. W. *J. Am. Chem. Soc.* **2002**, *124*, 4972−4973.
(11) Nowick, J. S.; Brower, J. O. *J. Am. Chem. Soc.* **2003**, *125*, 876−877.
(12) Woods, R. J.; Brower, J. O.; Castellanos, E.; Hashemzadeh, M.; Khakshoor, O.; Russu, W. A.; Nowick, J. S. *J. Am. Chem. Soc.* **2007**, *129*, 2548−2558.
(13) Mutants of macrocycle **1** are named as illustrated: $\mathbf{1}_{V1A}$ to reflect mutation of the valine at position R_1 to alanine and $\mathbf{1}_{K6L,L7K}$ to reflect double mutation of the lysine at position R_6 to leucine and the leucine at position R_7 to lysine.
(14) Time t_m is calculated as the halfway point between the final fluorescence and that of the ThS background fluorescence.
(15) In the experiments where the macrocycle substantially delays AcPHF6 aggregation, the t_m of the triplicate within one plate is extremely sensitive to small experimental variations, thus causing relatively large variations in t_m from well to well. The average t_m of the triplicate also varies from plate to plate when these experiments are repeated.
(16) A reviewer has thoughtfully pointed out that hydrophobic β-branched amino acids, such as valine, isoleucine, cyclohexylglycine, and alloisoleucine, are known to especially favor paired interstrand interaction through parallel β-sheet formation. For examples, see: (a) Toniolo, C.; Palumbo, M. *Biopolymers* **1977**, *16*, 219−224. (b) Toniolo, C. *Macromolecules* **1978**, *11*, 437−438 Favorable paired interstrand interactions of hydrophobic β-branched amino acids in parallel β-sheet formation could contribute to the effects observed for the R_1 and R_3 residues, although not for the effects observed for the R_7 residue.
(17) Takahashi, T.; Mihara, H. *Acc. Chem. Res.* **2008**, *41*, 1309−1318.
(18) Funke, S. A.; Willbold, D. *Curr. Pharm. Des.* **2012**, *18*, 755−767.
(19) Rojas Quijano, F. A.; Morrow, D.; Wise, B. M.; Brancia, F. L.; Goux, W. J. *Biochemistry* **2006**, *45*, 4638−4652.
(20) Moore, C. L.; Huang, M. H.; Robbennolt, S. A.; Voss, K. R.; Combs, B.; Gamblin, T. C.; Goux, W. J. *Biochemistry* **2011**, *50*, 10876−10886.